Spatial patterns of ecosystem carbon residence time in Chinese forests

ZHOU Tao[1,2*], SHI PeiJun[1,2], JIA GenSuo[3], LI XiuJuan[1,2] & LUO YiQi[4]

[1] *State Key Laboratory of Earth Surface Processes and Resource Ecology, Beijing Normal University, Beijing 100875, China;*
[2] *Academy of Disaster Reduction and Emergency Management, Ministry of Civil Affairs & Ministry of Education, Beijing 100875, China;*
[3] *Key Laboratory of Regional Climate-Environment Research for Temperate East Asia, Chinese Academy of Sciences, Beijing 100029, China;*
[4] *Department of Botany and Microbiology, University of Oklahoma, Norman, OK 73019, USA*

Capacity of carbon sequestration in forest ecosystem largely depends on the trend of net primary production (NPP) and the length of ecosystem carbon residence time. Retrieving spatial patterns of ecosystem carbon residence time is important and necessary for accurately predicting regional carbon cycles in the future. In this study, a data-model fusion method that combined a process-based regional carbon model (TECO-R) with various ground-based ecosystem observations (NPP, biomass, and soil organic carbon) and auxiliary data sets (NDVI, meteorological data, and maps of vegetation and soil texture) was applied to estimate spatial patterns of ecosystem carbon residence time in Chinese forests at steady state. In the data-model fusion, the genetic algorithm was used to estimate the optimal model parameters related with the ecosystem carbon residence time by minimizing total deviation between modeled and observed values. The results indicated that data-model fusion technology could effectively retrieve model parameters and simulate carbon cycling processes for Chinese forest ecosystems. The estimated carbon residence times were highly heterogenous over China, with most of regions having values between 24 and 70 years. The deciduous needleleaf forest and the evergreen needleleaf forest had the highest averaged carbon residence times (73.8 and 71.3 years, respectively), the mixed forest and the deciduous broadleaf forest had moderate values (38.1 and 37.3 years, respectively), and the evergreen broadleaf forest had the lowest value (31.7 years). The averaged carbon residence time of forest ecosystems in China was 57.8 years.

carbon residence time, carbon cycle, forest ecosystem, data-model fusion, inverse modeling, genetic algorithm

Rising atmospheric CO_2 concentration since the industrial revolution, due to fossil fuel combustion and land use change, has resulted in global warming, and triggered a series of environmental problems [1]. How to mitigate the increasing rate of atmospheric CO_2 effectively is not only a scientific issue but also a political and economic issue [2]. Forest re-growth (i.e., forest restoration after human and/or natural disturbances) and enhanced growth (i.e., growth enhancement due to 'fertilization effect' of CO_2 concentration, increased nitrogen deposition, and climate change) could effectively uptake atmospheric CO_2. Therefore, forest ecosystem is a significant carbon sink and has been extensively concerned by the communities [3]. As forest carbon sequestration could effectively uptake atmospheric CO_2 and alleviate intensity of global warming at low cost but high benefits [4, 5], researches on forest carbon sink have become important, especially after the enforcement of Kyoto Protocol [6, 7]. These researches include both the magni-

*Corresponding author (email: tzhou@bnu.edu.cn)

tude and the efficiency for carbon sink in forest ecosystems [3, 8].

Capacity of forest carbon sequestration depends mainly on two kinds of factors, i.e., the increase trend of net primary production (NPP) and the length of the ecosystem carbon residence time [9]. Forest re-growth and enhanced growth, accompanied by an increase trend of NPP, are external driving forces that make more atmospheric CO_2 enter forest tissues and be temporarily stored in the ecosystem. The ecosystem carbon residence time, however, is an intrinsic factor that determines the length of those fixed carbon and the efficiency of ecosystem carbon sequestration [9, 10]. The ecosystem carbon residence time is the averaged length of time a carbon atom can stay in plant and soil carbon pools from the entrance via photosynthesis to the release back to the atmosphere via plant and microbial respiration [11]. The value of ecosystem carbon residence time is determined by the residence times of sub-pools and the related transfer coefficients among those sub-pools [9, 11]. As a result, retrieving the spatial patterns of the ecosystem carbon residence time is quite important for understanding the mechanisms of carbon cycling and evaluating the potential of carbon sequestration [12, 13].

Due to rapid developments of remote sensing techniques and extensive applications of light-use efficiency models, the spatial patterns of NPP and its change trend have been relatively well quantified at regional and global scale [14–16]. Under this circumstance, the precision of the modeled ecosystem carbon sink depends primarily on the available information of spatial patterns of carbon residence time [9, 13]. Unfortunately, the spatial patterns of carbon residence time have not been quantified for Chinese forest ecosystems.

Several methods have been used to estimate the carbon residence times. One is an experimental approach that usually measures standing stock of a certain pool and the corresponding fluxes, and then uses the ratio of stock divided by flux as the approximation of residence times [17]. This traditional method is simple and easy to use, but the challenge is that not all standing stocks and fluxes can be easily measured (e.g., root mortality). The second is carbon isotope approach. Nuclear bomb tests in the 1960s caused a drastic increase of ^{14}C in the atmosphere. This so-called "bomb carbon" has been successively transferred from the atmosphere to plants and to soil organic carbon. Thus, the bomb carbon has been used as a tracer to estimate carbon residence times in various pools [18]. However, the residence times estimated from "bomb carbon" method for individual plant and soil pools have to be incorporated into models to estimate the ecosystem carbon residence times on regional scales. The third is inverse modeling approach that has recently become one major tool for data-model fusion [19]. The inverse modeling approach has been successfully applied to estimate carbon residence times at the ecosystem scale and the regional scale [9, 11–13].

This study is to estimate optimal model parameters, i.e., carbon residence times and related transfer coefficients of carbon pools, for Chinese forest ecosystems at steady state, based on the data-model fusion method that combines a process-based regional carbon model (TECO-R [13]), a genetic algorithm, and various ground-based observations.

1 Methods and data

1.1 Model structure

The data-model fusion conducted in this study was based on a Terrestrial ECOsystem Regional (TECO-R) model (Figure 1), which was developed by CASA light-use efficiency model [20, 21] and the Vegetation-And-Soil-Carbon-Transfer (VAST) model [11]. TECO-R model divided root biomass and soil organic carbon (SOC) into three soil layers. As TECO-R model depicted the basic processes of carbon transfer among pools, its model structure was suitable for all forest ecosystems on condition that appropriate model parameters that reflect forest-specific characteristics were applied. The key model parameters in TECO-R model included the maximum light-use efficiency (ε^*), carbon allocation coefficients among pools (α_L, α_W, α_R, ξ_{R_1}, ξ_{R_2}, ξ_{R_3}, θ_F, θ_C, η, θ_{S_1}, θ_{S_2}), and carbon residence times in individual plant and soil pools (τ_L, τ_W, τ_{R_1}, τ_{R_2}, τ_{R_3}, τ_F^*, τ_C^*, $\tau_{S_1}^*$, $\tau_{S_2}^*$, $\tau_{S_3}^*$). The detail information of those model parameters is listed in Table 1.

In TECO-R model, NPP is a function of the absorbed photosynthetically active radiation (*APAR*), maximum light-use efficiency (ε^*), and temperature and moisture stress scalars (T_ε, W_ε).

$$NPP = fAPAR \cdot PAR \cdot \varepsilon^* \cdot T_\varepsilon \cdot W_\varepsilon, \tag{1}$$

where *fAPAR* is a fraction of *PAR* that is absorbed by vegetation, which was determined by using a linear relationship with normalized difference vegetation index (NDVI) [22]. Thus, *APAR* equals *FAPAR* times *PAR*. *PAR* is estimated by observation of solar radiation (*Sr*), i.e., *PAR*=*Sr* × 0.5. In TECO-R model, we used the same scalars as CASA model for T_ε and W_ε [23].

The estimated NPP is allocated to plant tissues of leaves, stem, and roots according to the carbon allocation coefficients:

$$\mathrm{NPP}_L = \alpha_L \mathrm{NPP}, \tag{2}$$

$$\mathrm{NPP}_W = \alpha_W \mathrm{NPP}, \tag{3}$$

$$\mathrm{NPP}_R = \alpha_R \mathrm{NPP}, \tag{4}$$

Table 1 Symbol and definition of model parameters

Symbol	Definition	Lower erlimit	Upper limit	Unit	Constraint
ε^*	Maximum light-use efficiency	0.0	2.76	g C MJ^{-1}	
α_L	Allocation of NPP to leaves	0.0	1.0	Dimensionless	
α_W	Allocation of NPP to wood	0.0	1.0	Dimensionless	
α_R	Allocation of NPP to roots	0.0	1.0	Dimensionless	$\alpha_L + \alpha_W + \alpha_R = 1$
ξ_{R_1}	Allocation proportion of NPP for roots (0–20 cm)	0.0	1.0	Dimensionless	$\xi_{R_1} > \xi_{R_2} > \xi_{R_3}$
ξ_{R_2}	Allocation proportion of NPP for roots (20–50 cm)	0.0	1.0	Dimensionless	
ξ_{R_3}	Allocation proportion of NPP for roots (50–100 cm)	0.0	1.0	Dimensionless	$\xi_{R_1} + \xi_{R_2} + \xi_{R_3} = 1$
θ_F	Carbon partitioning coefficient of the fine litter pool	0.0	0.5	Dimensionless	
θ_C	Carbon partitioning coefficient of coarse litter pool	0.0	0.5	Dimensionless	
θ_{S_1}	Carbon partitioning coefficient of SOC (0–20 cm)	0.0	0.1	Dimensionless	
θ_{S_2}	Carbon partitioning coefficient of SOC (20–50 cm)	0.0	0.1	Dimensionless	
η	Fraction of mechanical breakdown for coarse litter pool	0.0	0.1	Dimensionless	
τ_L	Carbon residence time of leaves	0.0	10.0	Year	$\tau_L < \tau_W$
τ_W	Carbon residence time of wood	0.0	500.0	Year	
τ_{R_1}	Carbon residence time of roots (0–20 cm)	0.0	100.0	Year	
τ_{R_2}	Carbon residence time of roots (20–50 cm)	0.0	100.0	Year	
τ_{R_3}	Carbon residence time of roots (50–100 cm)	0.0	100.0	Year	
τ_F^*	Moisture and temperature corrected residence time of fine litter	0.2	2.0	Year	
τ_C^*	Moisture and temperature corrected residence time of coarse litter	0.5	5.0	Year	$\tau_C^* > \tau_F^*$
$\tau_{S_1}^*$	Moisture and temperature corrected residence time of SOC (0–20 cm)	0.0	100.0	Year	$\tau_{S_1}^* < \tau_{S_2}^* < \tau_{S_3}^*$
$\tau_{S_2}^*$	Moisture and temperature corrected residence time of SOC (20–50 cm)	0.0	250.0	Year	
$\tau_{S_3}^*$	Moisture and temperature corrected residence time of SOC (50–100 cm)	0.0	500.0	Year	
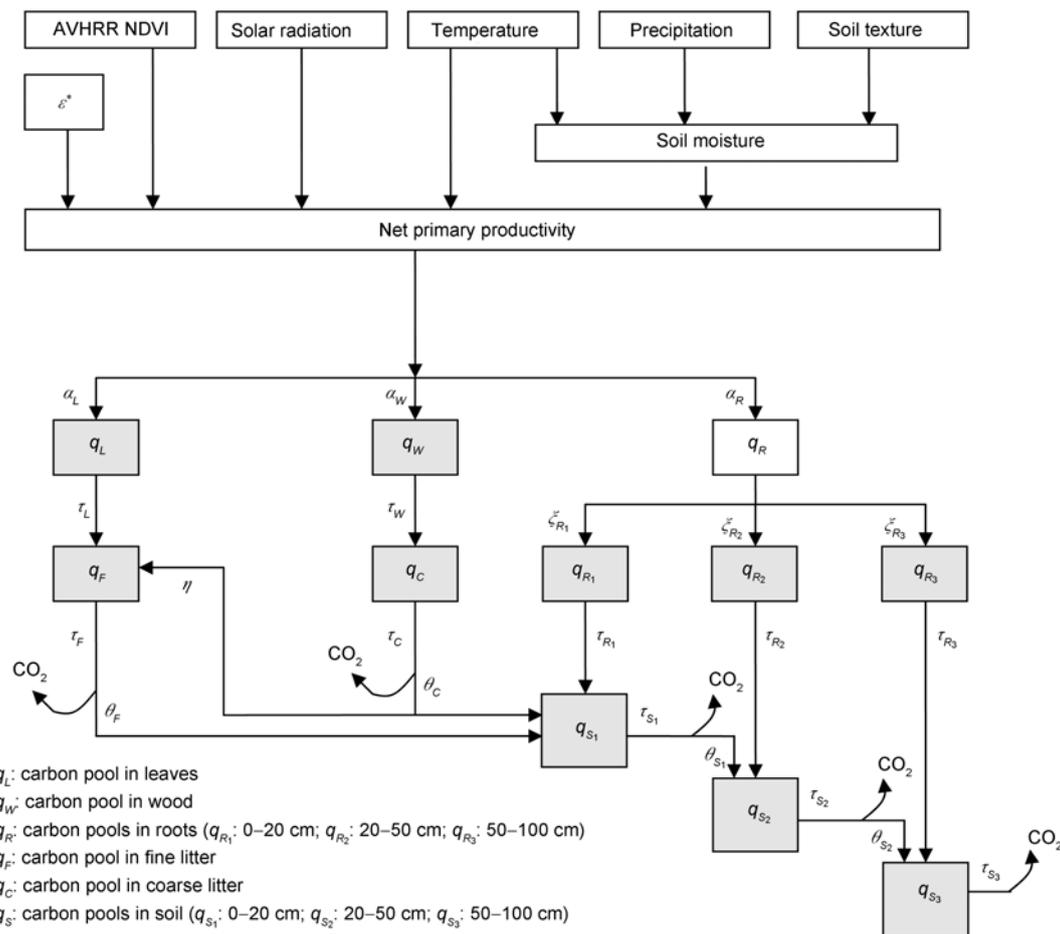
Figure 1 Structure of the terrestrial ecosystem regional model (TECO-R).

where α_L, α_W, and α_R are allocation coefficients of NPP for leaves, wood, and roots, respectively. Thus, the carbon dynamics in leaf stem and root pools can be described by

$$\frac{\mathrm{d}q_L}{\mathrm{d}t} = \alpha_L NPP - q_L / \tau_L, \tag{5}$$

$$\frac{\mathrm{d}q_W}{\mathrm{d}t} = \alpha_W NPP - q_W / \tau_W, \tag{6}$$

$$\frac{\mathrm{d}q_{R_j}}{\mathrm{d}t} = \xi_{R_j} \alpha_R NPP - q_{R_j} / \tau_{R_j}, \ j=1, \ 2, \ 3, \tag{7}$$

where q_L, q_W, and q_{R_j} are carbon pool sizes in leaves, wood, and roots, respectively; τ_L, τ_W, and τ_{R_j} are carbon residence times in the pools of leaves, wood, and roots, respectively; the subscript j ($j =1, 2, 3$) indicates three soil layers (0–20, 20–50, and 50–100 cm) for root biomass partitioning; and ξ_{R_j} are the partitioning coefficients of root biomass into three layers.

The carbon dynamics in the litter and soil organic carbon (SOC) pools are partially determined by carbon transferred from plant biomass and can be modeled by

$$\frac{\mathrm{d}q_F}{\mathrm{d}t} = q_L / \tau_L + \eta q_C / \tau_C - q_F / \tau_F, \tag{8}$$

$$\frac{\mathrm{d}q_C}{\mathrm{d}t} = q_W / \tau_W - q_C / \tau_C, \tag{9}$$

$$\frac{\mathrm{d}q_{S_1}}{\mathrm{d}t} = q_{R_1} / \tau_{R_1} + \theta_F q_F / \tau_F + \theta_C q_C / \tau_C - q_{S_1} / \tau_{S_1}, \tag{10}$$

$$\frac{\mathrm{d}q_{S_j}}{\mathrm{d}t} = q_{R_j} / \tau_{R_j} + \theta_{S_{j-1}} q_{S_{j-1}} / \tau_{S_{j-1}} - q_{S_j} / \tau_{S_j}, \ j=2, 3, \tag{11}$$

where q_F and q_C are carbon pool sizes for fine and coarse litter, respectively; q_{S_1}, q_{S_2}, and q_{S_3} are pool sizes of SOC in three soil layers, respectively; τ_F, τ_C, τ_{S_1}, τ_{S_2}, and τ_{S_3} are carbon residence times in fine litter, coarse litter, and SOC in three layers, respectively; η is a fraction of C exiting the coarse woody debris pool by mechanical break down; θ_F and θ_C are carbon partitioning coefficients of the fine litter and coarse litter pools, respectively; θ_{S_1} and θ_{S_2} are partitioning coefficients of SOC in the first and second soil layers, respectively.

Carbon residence times of litter and SOC pools (τ_F, τ_C, τ_{S_1}, τ_{S_2}, and τ_{S_3}) are impacted by climatic factors, soil properties, and vegetation type [24]. Decomposition rates of litter and soil organic matter are controlled primarily by

properties of soil microbe, which is highly related with site-specific climatic factors and soil properties. Forest type also significantly affects carbon residence times. On the one hand, plant tissues (i.e., leaf, stem, and roots pools) of different forest types have apparent differences on residence times. On the other hand, plant's litters (i.e., fine litter and coarse litter pools) of different forests have different chemical compositions (e.g., ratio of lignin to nitrogen), which affects the decomposition rates of litter pools [20]. To reflect potential influences of forest types on parameters estimation, TECO-R model divided Chinese forest into five types, evergreen broadleaf forest (EBF), deciduous broadleaf (DBF), evergreen needleleaf forest (ENF), deciduous needleleaf forest (DNF), and mixed forest (MF), based on 1:4000000 vegetation map provided by Data Sharing Infrastructure of Earth System Science (http://www.geodata.cn). The optimal model parameters were separately estimated for different forest types. To quantify potential influences caused by spatial heterogeneity of climatic factors, TECO-R model relates the site-specific residence times (τ_F, τ_C, τ_{S_1}, τ_{S_2}, and τ_{S_3}) to the temperature and moisture corrected residence times (τ^*_F, τ^*_C, $\tau^*_{S_1}$, $\tau^*_{S_2}$, and $\tau^*_{S_3}$) by

$$\tau_k = \tau^*_k / (W_s \cdot T_s), \ k = F, \ C, \ S_1, \ S_2, \ S_3, \tag{12}$$

where W_s and T_s are temperature and moisture scalars for site-specific carbon residence times. The moisture scalar (W_s) is estimated by monthly precipitation (PPT), potential evapotranspiration (PET) and soil moisture (SoilM) simulated by CASA soil moisture submodel [23]:

$$SM = \frac{\mathrm{PPT} + \mathrm{SoilM}}{\mathrm{PET}}, \tag{13a}$$

$$W_s = 0.1 + 0.9 SM, \ 0 \leqslant SM \leqslant 1, \tag{13b}$$

$$W_s = 1.0, \ 1 < SM \leqslant 2, \tag{13c}$$

$$W_s = [1.0 + (1.0/28.0)] - (0.5/28.0)SM, \ 2 < SM \leqslant 30, \tag{13d}$$

$$W_s = 0.5, \ 30 \leqslant SM. \tag{13e}$$

The temperature scalar of decomposition, T_s, was obtained directly from monthly temperature data (T), as in Century soil-carbon model [25]:

$$T_s = \begin{cases} 1/(1+19\mathrm{e}^{-0.16T}), & T < 45°\mathrm{C}, \\ 10 - 0.2T, & 45 \leqslant T \leqslant 50°\mathrm{C}, \\ 0, & T > 50°\mathrm{C}. \end{cases} \tag{14}$$

As most of observation data sets used for parameters estimation (i.e., NPP, biomass, and SOC) were on the yearly scale, the model parameters in TECO-R, i.e., allocation coefficients and residence times of pools, estimated by

data-model fusion were on the yearly scale, too. The yearly NPP, however, was summed up by monthly NPP modeled by the light-use efficiency model, in which monthly NDVI, temperature, precipitation, and solar radiation were applied as input data.

1.2   Data

In this study, 13 observed data sets were used, which included three NPP data sets [26] (i.e., NPP in leaves, stems, and roots), each containing 228 data points; five biomass data sets [26] (i.e., one for biomass of leaves, one for stems, and three for roots in three soil layers), each containing 228 data points; two litter data sets (i.e., fine litter and coarse litter pools) provided by Chinese Ecosystem Research Network, each containing 10 data points; and three SOC data sets in the three soil layers [27, 28], each containing 62 data points. Among those 13 data sets, 11 data sets of NPP, biomass, and SOC were used for parameters estimation, where the other 2 data sets of fine litter and coarse litter were used for verification. The spatial distribution of those observation data points illustrated in Figure 2. Because the goal of this study was to estimate the spatial patterns of ecosystem carbon residence time at steady state, the data points selected for parameters estimation came from the mature forests where they suffered fewer human and natural disturbances, with forest ages larger than 80 years for DBF and larger than 100 years for the others (i.e., EBF, ENF, DNF, and MF).

Sources of auxiliary data used in this study were (1) the AVHRR-NDVI continental subsets of 8-km spatial resolution from 1982 to 1999 available from the Data and Infor-mation Services Center of Goddard Earth Science; (2) data sets of monthly solar radiation, temperature, and precipitation of 1-km spatial resolution [29]; (3) 1:14000000 soil texture map of China [30]; (4) 1:4000000 vegetation map of China available from Data Sharing Infrastructure of Earth System Science (http://www.geodata.cn). All those auxiliary data sets were resampled to a common projection (Lat-Long Projection) and spatial resolution (0.08°). Given the discrepancies of ground-based observations on sampling time and the influences of interannual variability of climatic factors and NDVI on modeling of NPP and biomass, the values of NDVI and climatic factors used for parameters estimation were multi-years monthly means.

1.3   Parameter estimation

The parameter estimation was based on the weighted least squares principle that minimized the deviations between the modeled and observed values for each of the five forest types. Given one forest type, we defined a partial cost function j_m as the sum of squares of deviations between observed and modeled values for data set m:

$$j_m = \sum_{n=1}^{N_m} [y_{nm} - \hat{y}_{nm}(x_n, \mathbf{a})]^2, \qquad (15)$$

where y_{nm} is the nth observed data point in the mth data set; $\hat{y}_{nm}(x_n, \mathbf{a})$ is the modeled value that corresponds to the observation y_{nm}. N_m is the total data points in mth data set; x_n is an auxiliary forcing vector that includes NDVI, solar radiation, temperature, precipitation, and soil texture, in a spatial grid where the nth observation was made; and $\mathbf{a}$ is a
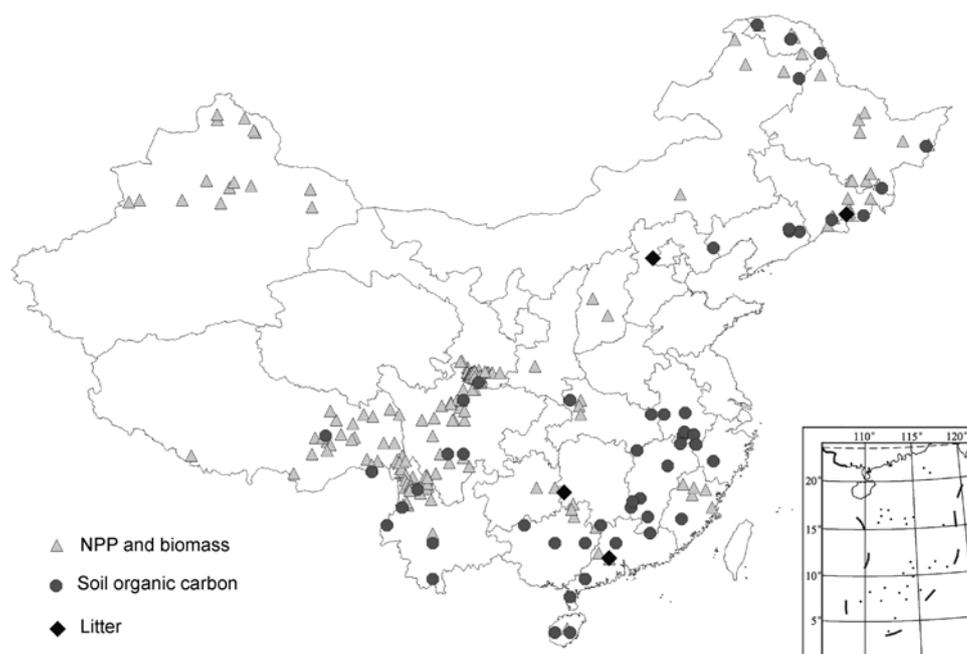
Figure 2   Spatial distribution of the observed data.

vector of parameters: $\mathbf{a} = \{ \varepsilon^*,\ \alpha_L,\ \alpha_W,\ \alpha_R,\ \xi_{R_1},\ \xi_{R_2},$ $\xi_{R_3},\ \tau_L,\ \tau_W,\ \theta_F,\ \theta_C,\ \eta,\ \tau_{R_1},\ \tau_{R_2},\ \tau_{R_3},\ \tau_F^*,\ \tau_C^*,$ $\tau_{S_1}^*,\ \tau_{S_2}^*,\ \tau_{S_3}^*,\ \theta_{S_1},\ \theta_{S_2} \}$. Each of the parameters is described in Table 1. A particular data set may provide information to constrain a subset of parameters. For example, the data set of leaf NPP directly constrains the parameters of ε^*, α_L, and τ_L. When all data sets are used, all parameters can be constrained by multiple data sets. In this case, an integrated cost function, J, can be expressed by

$$ J = \sum_{m=1}^{M} \lambda_m \left\{ \sum_{n=1}^{N_m} [y_{nm} - \hat{y}_{nm}(x_n, \mathbf{a})]^2 \right\},\ m = 1,\ 2,\ \cdots,\ M,\ (16) $$

where λ_m is a weighing factor of the partial cost j_m, which is inversely proportional to the variance of each data set [9].

To estimate the globally optimal parameters, the genetic algorithm (GA) was used in this study [31]. The steps of searching for the globally optimal parameters were (1) initializing the parameter vector, $\mathbf{a}$, from the parameter ranges with random numbers; (2) applying genetic algorithm (selection, crossover, and mutation) to generate the new offspring of parameter values of $\mathbf{a}$; (3) using the generated parameter values in eqs. (2)–(11) to calculate the modeled values of NPP and carbon pools under a steady state assumption (i.e., the $\mathrm{d}q_i/\mathrm{d}t = 0$, i stands for each sub-pool in Figure 1) , and then calculate partial cost functioin j_m; (4) calculating the integrated cost function J; and (5) judging stopping condition of evolution (change of J in last 100 offspring less than 0.001%). If the stopping criterion was satisfied, then the algorithm exported the optimal parameters. Otherwise, it went to step (2) to continue the search.

The estimated carbon residence times and allocation coefficients for individual C pools in plant tissues and soils were used to calculate the aggregated ecosystem carbon residence time using eq. (17) [11]:

$$ \begin{aligned} \tau_E =\ & \alpha_L(\tau_L + \tau_F) + \eta \alpha_W \tau_F + \alpha_W(\tau_W + \tau_C) \\ & + \alpha_R[\xi_{R_1}(\tau_{R_1} + \tau_{S_1}) + \xi_{R_2}(\tau_{R_2} + \tau_{S_2}) + \xi_{R_3}(\tau_{R_3} + \tau_{S_3})] \\ & + F_1 \tau_{S_1} + F_2 \theta_{S_1} \tau_{S_2} + F_3 \theta_{S_2} \tau_{S_3}, \end{aligned} \quad (17) $$

where

$$ \begin{aligned} F_1 &= \theta_F(\alpha_L + \eta \alpha_W) + \theta_C \alpha_W, \\ F_2 &= \alpha_R \xi_{R_1} + F_1, \\ F_3 &= \alpha_R \xi_{R_2} + \theta_{S_1} F_2. \end{aligned} \quad (18) $$

We ran the optimization algorithm for 30 times to obtain means and standard deviations of the estimated parameters. Estimated standard deviation reflected integration of model errors, data errors, and errors in the data-model fusion technique [13].

1.4 Sensitivity analysis

Because of the lack of well-documented time serials of data on NPP, plant biomass, and SOC in most of the ecosystems, this study was unable to estimate residence times and initial values of pool size to assess nonsteady state carbon dynamics [32]. To examine potential influences of the steady state assumption on the values of estimated residence times, we conducted a sensitivity analysis for the forest type of EBF to estimate nonsteady state carbon residence times. In the sensitivity analysis, we assumed that EBF is a carbon sink, that is, ecosystem carbon input through NPP is larger than ecosystem carbon output through heterotrophic respiration. In the analysis, we set five scenarios of carbon sink, i.e., the amounts of carbon sink equal 2%, 6%, 10%, 15%, and 20% of NPP, respectively.

As measurement errors of observation data also affect the precision of the estimated parameters [19], we conducted a sensitivity analysis for forest type EBF to assess the sensitivity of the estimated parameters to measurement errors. Eight scenarios were used in this study; each scenario assumed only one observation data set being overestimated by 20%, respectively. The observation data sets in eight scenarios included (1) leaf NPP; (2) stem NPP; (3) root NPP; (4) leaf biomass; (5) stem biomass; (6) SOC in 0–20 cm; (7) SOC in 20–50 cm; and (8) SOC in 50–100 cm.

2 Results

2.1 Comparisons between modeled and observed data

To evaluate the validity of the data-model fusion method, we conducted some comparisons between modeled and observed data. The verifications were reviewed from two aspects. One is for rationality of model structure and parameter values. That is, with 22 optimized parameters, if the TECO-R model could effectively simulate processes of carbon cycling and, accordingly, made the modeled values consistent with the corresponding observations. The other one is for rationality of the estimated carbon residence times for litter pools. Although the observation data sets of fine litter and coarse litter were not used as constraints for parameters estimation, the estimated residence times of litter pools by data-model fusion should be consistent with those by traditional method (standing stock of litter/annual litterfall), on condition that the data-model method is effectual.

The results showed that the modeled values (i.e., NPP, biomass, and SOC) were closely related to the observed data when the estimated optimal parameters were used in the model (Figure 3), which indicated that the model structure and parameters as well as the data-model fusion method were feasible to simulate carbon cycling of forest ecosystems in China. In addition, the results disclosed that although the observed litter pools were not used as constraints, their residence times estimated by data-mode fusion

were also reasonable and matched with those obtained by the traditional method (Figure 4). One of distinguished advantages for data-model fusion is that when the information contained in process-based model was used, what could be estimated include not only the parameters directly constrained by the observations but also the ones indirectly related with those observations.

2.2 Maximum of light-use efficiencies

Maximum of light-use efficiency (ε^*) is a key parameter because it reflects potential productivity and, accordingly, influences the amount of carbon that enters into ecosystem and the subsequent transfer processes. The results in Table 2 and Figure 5(a) indicated that the evergreen broadleaf forest
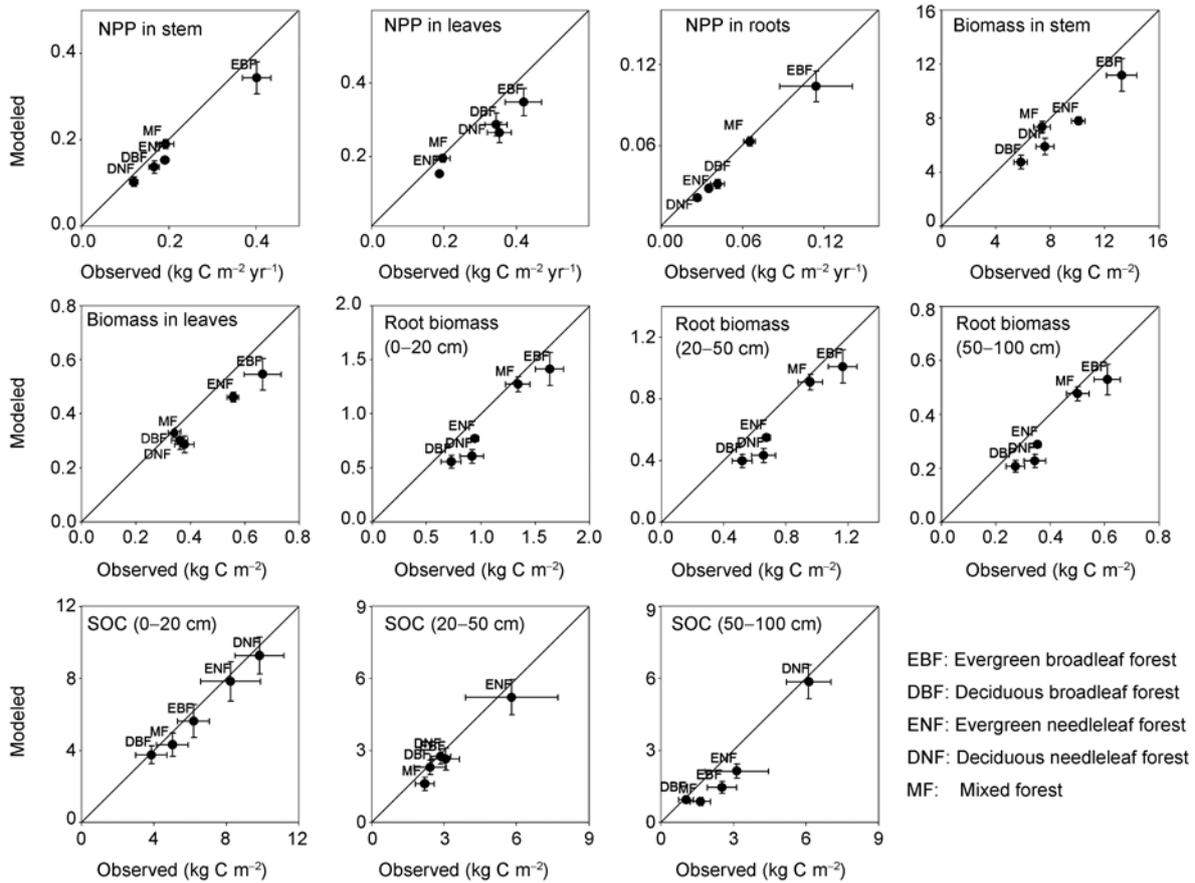
Figure 3 Comparisons between observed and modeled values. Points in each panel represent means of forests with horizontal and vertical standard error bars to indicate variations among observed and modeled values, respectively.
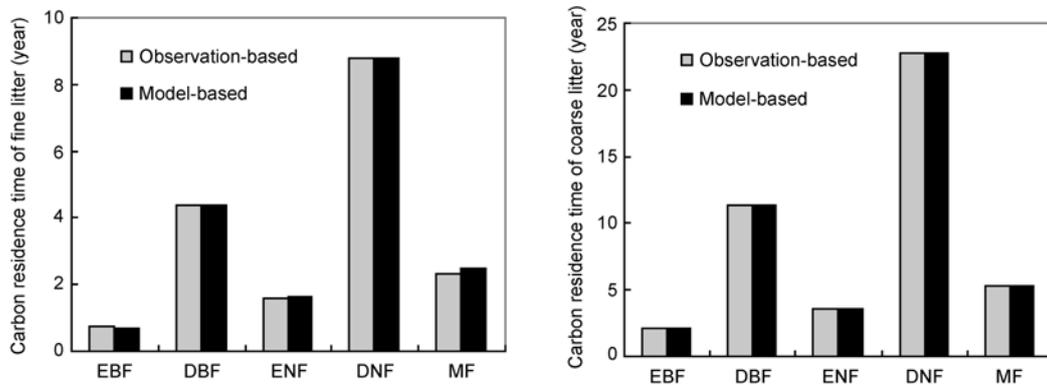
Figure 4 Comparisons of carbon residence times for litter pools (τ_F and τ_C) between the model-based estimations and observation-based estimations (standing stock of litter/annual litterfall).

Table 2   Comparisons of maximum of light-use efficiencies among different studies

	This study [a]	Zhu et al. [34] [b]	Peng et al. [35]	Running et al. [33][c]
Evergreen broadleaf forest (EBF)	1.20	0.985	1.25	1.259
Deciduous broadleaf forest (DBF)	0.57	0.692		1.044
Evergreen needleleaf forest (ENF)	0.44	0.389		1.008
Deciduous needleleaf forest (DNF)	0.57	0.485		1.103
Mixed forest (MF)	0.47	0.475		

a) Integrated various observations information (i.e., NPP, biomass, and SOC) and TECO-R model information. b) Based purely on NPP observations. c) Based on physiological and ecological model (BIOME-BGC). Unit: g C MJ^{-1}.

had the highest light-use efficiency (1.20 g C MJ^{-1}); the deciduous broadleaf forest and the deciduous needleleaf forest had the moderate values (0.57 g C MJ^{-1}); and the evergreen needleleaf forest and mixed forest had the lowest values (0.44 and 0.47 g C MJ^{-1}, respectively). The relative magnitudes of light-use efficiencies in this study were comparable with other studies by Running et al. [33] and Zhu et al. [34] (Table 2). For instance, all studies indicated that the evergreen broadleaf forest had the highest light-use efficiency, which followed by the deciduous broadleaf forest and the deciduous needleleaf forest, whereas the mixed forest and evergreen needleleaf forest had the lowest light-use efficiencies.

The estimated light-use efficiencies in this study were more similar to those derived purely from NPP observations by Zhu et al. [34] (Table 2), except for the evergreen broadleaf forest. The maximum of light-use efficiency for evergreen broadleaf forest is 1.20 g C MJ^{-1}, apparently higher than 0.985 g C MJ^{-1} by Zhu et al. [34] but similar to 1.25 g C MJ^{-1} by Peng et al. [35] and 1.259 g C MJ^{-1} by Running et al. [33]. This result supported a conclusion by Peng et al. [35]; if the default parameter value of 0.389 g C MJ^{-1} in CASA [20, 21] was used, the model would significantly underestimate NPP of evergreen broadleaf forest in China.

2.3   Carbon residence times in plant biomass, litter, and soil pools

The leaf residence times estimated from data-model fusion were from 1.05 to 2.98 years (Figure 5(f)). The deciduous broadleaf and needleleaf forests had the lowest values (1.05 and 1.13 years, respectively), whereas the evergreen needleleaf forest had the highest value (2.98 years). The evergreen broadleaf forest and the mixed forest had moderate leaf residence times (1.63 and 1.70 years, respectively). The estimated carbon residence times of stem pools ranged from 32.14 to 56.64 years; the evergreen and deciduous broadleaf forests had the lowest values (32.14 to 34.57 years, respectively), whereas the evergreen and deciduous needleleaf forests had the highest values (51.42 and 56.64 years, respectively) and the mixed forest had a moderate value (38.36 years).

The root residence times of five forests were illustrated

in Figure 5(e). The evergreen and deciduous broadleaf forests had the lowest values, with 25.60 and 33.81 years in top soil layer (0–20 cm), 32.84 and 33.99 years in middle soil layer (20–50 cm), and 33.38 and 59.96 years in the bottom soil layer (50–100 cm). The evergreen and deciduous needleleaf forests had the highest values, with 55.79 and 56.79 years in top layer, 56.08 and 56.65 years in middle layer, and 57.25 and 57.82 years in the bottom layer. The mixed forest had the moderate root residence times, with the values of 37.64, 43.67, and 72.75 years, respectively, for the top, middle, and bottom soil layers.

The temperature- and moisture-corrected carbon residence times for litter and SOC were plotted in Figure 5(g) and (h). The estimated carbon residence times for fine litter (τ_F^*) were 0.27 to 1.42 years. The evergreen broadleaf and needleleaf forests had the lowest values (0.27 and 0.29 years, respectively), whereas the deciduous needleleaf forest had the highest value (1.42 years), and the deciduous broadleaf forest and the mixed forest had moderate values (0.91 and 0.90 years, respectively). The estimated temperature- and moisture-corrected carbon residence times for coarse litter (τ_C^*) were lowest for the evergreen broadleaf and needleleaf forests (0.65 and 0.68 years, respectively). The values of τ_C^* was the highest for the deciduous needleleaf forest (2.94 years). The deciduous broadleaf forest and the mixed forest had the moderate τ_C^* (1.89 and 1.53 years, respectively). The estimated temperature- and moisture-corrected carbon residence times of SOC ($\tau_{S_1}^*$, $\tau_{S_2}^*$, $\tau_{S_3}^*$) were much higher than those for litters (Figure 5(h)), ranging from 7.21 to 16.94 years for the top soil layer, from 13.13 to 81.21 years for the middle layer, and from 26.99 to 95.86 years for the bottom layer. For the top soil layer, the deciduous broadleaf and needleleaf forests had the lowest $\tau_{S_1}^*$ (7.38 and 7.21 years, respectively) whereas the evergreen needleleaf forest had the highest value (16.94 years). For the middle soil layer, the deciduous needleleaf forest had the lowest $\tau_{S_2}^*$ (13.13 years) whereas the evergreen needleleaf forest had the highest value (81.21 years); the evergreen and deciduous broadleaf forests and the mixed forest had the moderate values (22.02, 22.47, and
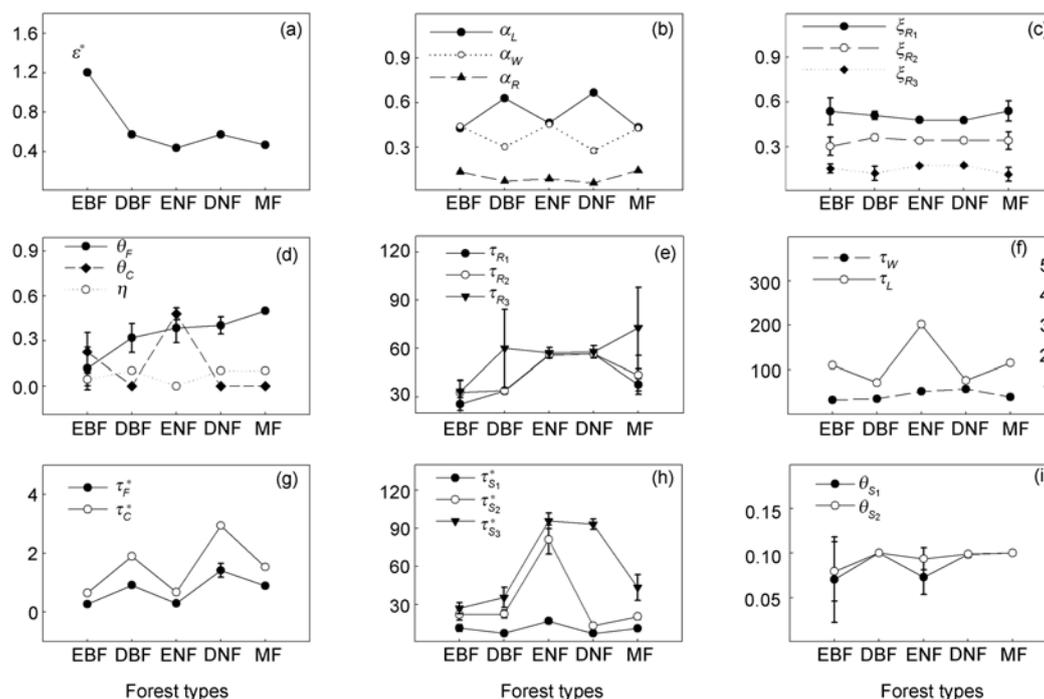
Figure 5 Optimized values of 22 parameters for five forests estimated by genetic algorithm. Symbols and units for the 22 parameters were described in Table 1.

20.45 years, respectively). For the bottom soil layer, the evergreen broadleaf forest had the lowest $\tau_{S_3}^*$ (26.99 years) whereas evergreen needleleaf forest had the highest value (93.15 years); the deciduous broadleaf forest and the mixed forest had the moderate values (35.62 and 43.15 years, respectively).

Because of spatial heterogeneities of the temperature and moisture, the actual residence times of litter and soil (τ_k) were different from the temperature- and moisture-corrected residence times (τ_k^*). If the influences of the temperature and moisture were considered (eqs. (12) to (14)), the actual residence times of fine litter ranged from 0.71 to 8.80 years (Figure 4). The deciduous needleleaf and broadleaf forests had the highest values (8.80 and 4.38, respectively), which followed by the mixed forest (2.50 years). The evergreen broadleaf and needleleaf forests had the lowest values (0.71 and 1.65 years, respectively). The actual residence times for coarse litter ranged from 2.07 to 22.76 years. For the same forest type, the residence times of coarse litter was significantly higher than that of fine litter. For the different forest types, coarse and fine litter had a similar relative magnitude, that is, the deciduous needleleaf forest > the deciduous broadleaf forest > the mixed forest > the evergreen needleleaf forest > the evergreen broadleaf forest.

2.4 Spatial patterns of forest ecosystem residence time

The carbon residence times of the whole forest ecosystem

(i.e. means of plant, litter, and SOC pools) in China were highly heterogeneous. The ecosystem residence times ranged from 24 to 100 years for most of spatial grids, especially from 24 to 70 years (Figure 6). The ecosystem carbon residence times trended to increase with latitude, as affected by the spatial patterns of temperature factor (T_s) and moisture factor (W_s). Because all forests have the relatively good moisture condition, the spatial patterns of temperature had a stronger influence on the spatial patterns of ecosystem carbon residence time.

When the spatial heterogeneities of temperature and moisture were considered, the statistic results of ecosystem residence times for five forests indicated that the deciduous needleleaf forest and evergreen needleleaf forest had the highest averaged values of 73.8 years (ranging from 48.3 to 172.6 years) and 71.3 years (ranging from 52.5 to 425.5 years), respectively. The mixed forest and the deciduous broadleaf forest had the moderate averaged values, which were 38.1 years (ranging from 33.9 to 162.7 years) and 37.3 years (ranging from 24.2 to 103.6 years), respectively. The evergreen broadleaf forest had the lowest averaged value, with a mean of 31.7 years and ranging from 27.4 to 221.8 years. For entire China, the averaged carbon residence time for all forest ecosystems was 57.8 years, with the values ranging from 24.2 to 425.5 years.

2.5 Sensitivity analysis

When ecosystems were in nonsteady state and the
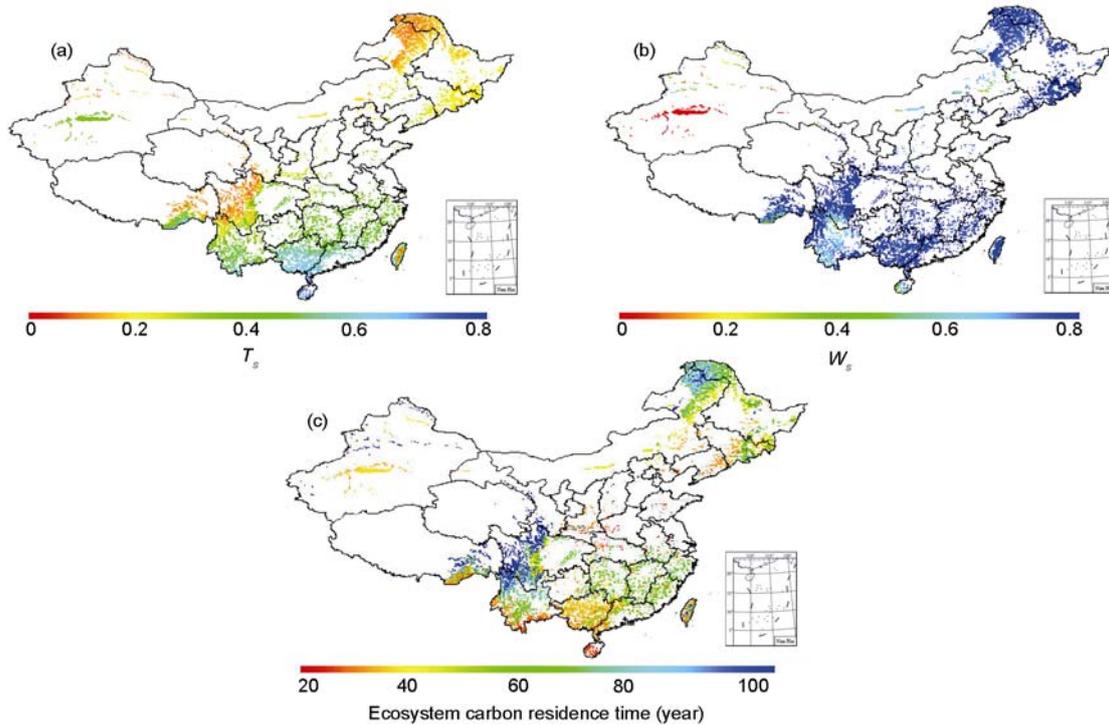
Figure 6 Spatial patterns of ecosystem carbon residence time estimated by data-model fusion.

magnitude of carbon sink varied from 0 to 20% of the total NPP, the estimated residence times had an increasing trend (Figure 7). That is, if the ecosystem were carbon sink, the estimated carbon residence times under the steady state assumption would potentially underestimate the value of residence times. However, the magnitude of carbon sink was usually much smaller than that of NPP if there did not experience rapid land cover modifications and significant disturbances, such as forest fires. For instance, the efficiency of carbon sink (i.e., magnitude of carbon sink for unit NPP) for Chinese evergreen broadleaf forest was just 2.6% [3], which only made the estimated carbon residence time 3% higher than that estimated by the steady state assumption (Figure 7). Therefore, the steady state assumption could not significantly affect the spatial patterns of ecosystem carbon residence time for Chinese forests.

When NPP, biomass, and SOC increased by 20%, the cost function, J, and the majority of the parameters did not change much and were usually less than 5% (Figure 8). In addition, the sensitivity analysis of observation errors on parameters estimation disclosed two characteristics. One is that a certain observation error usually significantly influences those parameters directly constrained by this observation. For instance, the allocation coefficient (α_L) and residence time for leaves (τ_L) were somewhat sensitive to changes in leaf NPP, while residence times of SOC (τ_S^*) were sensitive to changes in SOC observations. The other one is that the estimated residence time of fine litter (τ_F^*) and coarse litter (τ_C^*) showed relatively higher sensitivities

(Figure 8), when the observations of fine litter and coarse litter were not used as constraints during the parameters estimation.

3 Discussions

Under the condition that both observed flux and storage for a certain carbon pool were available, the carbon residence time was traditionally estimated by the ratio of storage to flux [17]. In this study, we applied a new method of data-model fusion by combining the process-base model with ground-based observations to estimated carbon residence times. Although this method was different from the traditional one, we found that the estimated parameter values were well consistent with those estimated by the traditional method. For instance, the estimated leaf carbon residence times for five forests (Figure 2) by the traditional method were 1.59, 1.05, 2.97, 1.07, and 1.73 years, respectively, which were highly consistent with those estimated by data-model fusion method in this study, with values of 1.60, 1.05, 2.98, 1.13, and 1.70 years. Similarly, the estimated stem carbon residence times (Figure 2) by traditional method were 33.02, 35.02, 52.77, 63.40, and 38.53 years, which were also consistent with those by data-model fusion method, with the values of 32.14, 34.57, 51.42, 56.64, and 38.36 years. Due to the significant advantage of information integration, the data-model fusion method could effectively estimate the optimal parameters and then simulate the processes of carbon cycling (Figure 3).
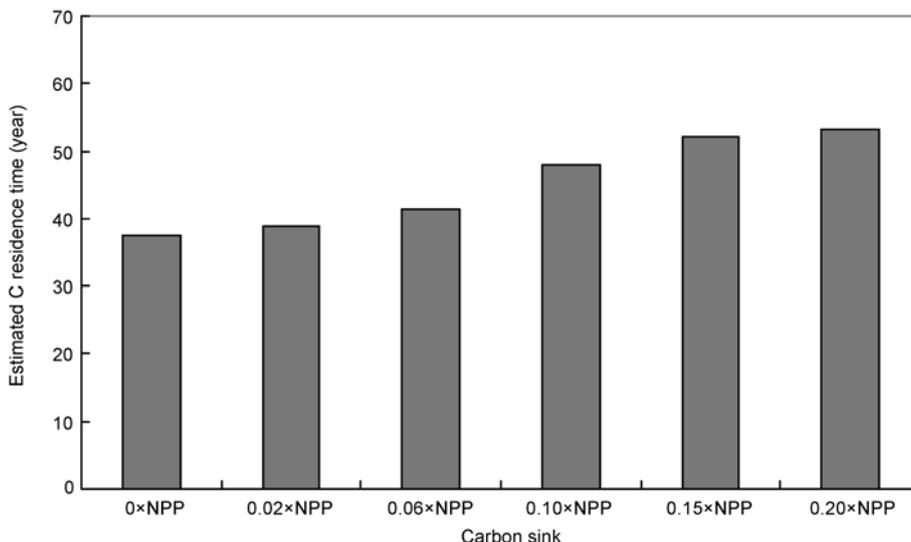
Figure 7 Sensitivity analysis of the estimated carbon residence times in nonsteady states. Estimated carbon residence times increase as the magnitude of carbon sink of 0, 2%, 6%, 10%, 15%, 20% of the total NPP.
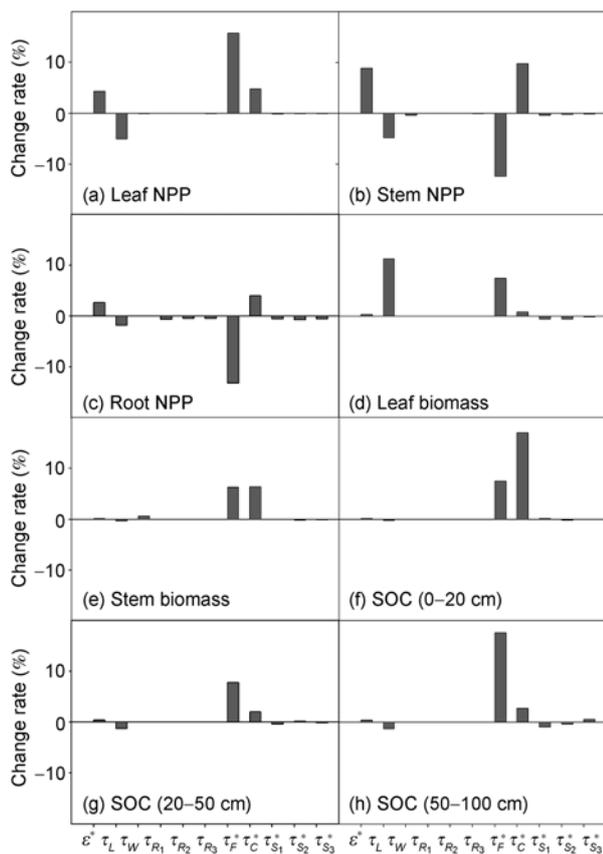
Figure 8 Sensitivity analyses of observation errors on estimated parameters. Each scenario corresponds to a certain observation error (overestimate of 20%). Note that cost function J and parameters ξ_{R_1}, ξ_{R_2}, and ξ_{R_3} were not plotted here because they did not vary much in response to changes of observed data.

Although both methods, traditional method and data-model fusion method, could be used to estimate parameters

of carbon residence times, the latter has some remarkable advantages. First, the traditional method needs to measure both storage and flux of a certain carbon pool at the same time, which is not always available. The data-model fusion method, however, not only could be used to reveal the parameters that can be measured through experiments but also the parameters that are not observable or difficult to observe from experiments [19]. Second, the processes of carbon cycling are dependent on both carbon residence times and the related parameters of carbon allocation that are usually hard to obtain directly from observations but could commonly be retrieved from data-model fusion method [9, 12]. Third, each observation inevitably has measurement errors. The data-model fusion method will synthetically analyze all errors contained in all data sets and therefore reduce influences of a certain observation error. As a result, the parameters estimated by data-model fusion are the optimal ones that make the total modeled error minimal.

4 Conclusions

In this study, we used the data-model fusion method, which included a process-based model (TECO-R), a genetic algorithm, and various ground-based observations, to estimate the spatial patterns of the carbon residence time in Chinese forests. The results indicated that data-model fusion method could effectively estimate the parameters and disclose the mechanisms of carbon cycling in Chinese forests. The estimated residence times were highly heterogeneous over the forests in China, with most of the regions having values from 24 to 70 years. For different forest types, the deciduous needleleaf forest and the evergreen needleleaf forest had the highest ecosystem carbon residence times; the mixed

forest and deciduous broadleaf forest had the moderate values; and the evergreen broadleaf forest had the lowest value. The averaged ecosystem carbon residence time for the entire Chinese forests was 57.8 years.

1   Solomon S, Qin D, Manning M, et al. Climate Change 2007: The Physical Science Basis. New York: Cambridge University Press, 2007

2   Young L M. Carbon sequestration in agriculture: The U.S. policy context. Am J Agr Econ, 2003, 85: 1164–1170

3   Fang J Y, Guo Z D, Piao S L, et al. Terrestrial vegetation carbon sinks in China, 1981−2000. Sci China Ser D-Earth Sci, 2007, 50: 1341–1350

4   Andrasko K. Climate Change and Global Forests: Current Knowledge of Potential Effects, Adaption and Mitigation Options. Rome: FAO Forestry Department, 1990

5   Brown S, Sathaye J, Cannell M, et al. Management of forests for mitigation of greenhouse gas emissions. In: Watson R T, Zinyowera M C, Moss R H, eds. Climate Change 1995: Impacts, Adaptations and Mitigation of Climate Change. Cambridge: Cambridge University Press, 1996. 773–798

6   Cannell M G R, Milne R, Haigreaves K J, et al. National inventories of terrestrial carbon sources and sinks: The UK experience. Clim Change, 1999, 42: 505–530

7   Dai M H, Zhai W D, Lu Z M, et al. Regional studies of carbon cycles in China: Progress and perspectives (in Chinese). Adv Earth Sci, 2004, 2: 120–130

8   Canadell J G, Corinne L Q, Raupach M R, et al. Contributions to accelerating atmospheric CO_2 growth from economic activity, carbon intensity, and efficiency of natural sinks. Proc Natl Acad Sci, 2007, doi: 10.1073/pnas.0702737104

9   Luo Y, White L, Josep G, et al. Sustainability of terrestrial carbon sequestration: A case study in Duke Forest with inversion approach. Glob Biogeochem Cycle, 2003, 17: 1021, doi: 10.1029/2002GB 001923

10 Luo Y, Wu L, Andrews A, et al. Elevated CO_2 differentiates ecosystem carbon processes: Deconvolution analysis of Duke forest FACE data. Ecol Monogr, 2001, 71: 357–376

11 Barrett D J. Steady state turnover time of carbon in the carbon in the Australian terrestrial biosphere. Glob Biogeochem Cycle, 2002, 16: 1108, doi: 10.1029/2002GB001860

12 Xu T, White L, Hui D, et al. Probabilistic inversion of a terrestrial ecosystem model: Analysis of uncertainty in parameter estimation and model prediction. Glob Biogeochem Cycle, 2006, 20: GB2007, doi: 10.1029/2005GB002468

13 Zhou T, Luo Y. Spatial patterns of ecosystem carbon residence time and NPP-driven carbon uptake in the conterminous United States. Glob Biogeochem Cycle, 2008, 22: GB3032, doi: 10.1029/2007GB 002939

14 Hicke J A, Asner G P, Randerson J T, et al. Trends in North American net primary productivity derived from satellite observations, 1982–1998. Glob Biogeochem Cycle, 2002, 16: 1018, doi: 10.1029/ 2001GB001550

15 Nemani R R, Keeling C D, Hashimoto H, et al. Climate-driven increases in global terrestrial net primary production from 1982 to 1999. Science, 2003, 300: 1560–1563

16 Piao S, Fang J, Zhou L M, et al. Changes in vegetation net primary productivity from 1982 to 1999 in China. Glob Biogeochem Cycle, 2005, 19: GB2027, doi: 10.1029/2004GB002274

17 Vogt K A, Vogt D J, Palmiotto P A, et al. Review of root dynamics in forest ecosystems grouped by climate, climatic forest type and species. Plant Soil, 1996, 187: 159–219

18 Gaudinski J B, Trumbore S E, Davidson E A, et al. The age of fine-root carbon in three forests of the eastern United States measured by radiocarbon. Oecologia, 2001, 129: 420–429

19 Raupach M R, Rayner P J, Barrett D J, et al. Model-data synthesis in terrestrial carbon observation: Methods, data requirements and data uncertainty specification. Glob Change Biol, 2005, 11: 378–397

20 Potter C S, Randerson J T, Field C B, et al. Terrestrial ecosystem production: A process model based on global satellite and surface data. Glob Biogeochem Cycle, 1993, 7: 811–841

21 Field C B, Randerson J T, Malmstrom C M. Global net primary production: Combining ecology and remote sensing. Remote Sens Environ, 1995, 51: 74–88

22 Ruimy A, Saugier B. Methodology for estimation of terrestrial net primary production from remotely sensed data. J Geophys Res, 1994, 97: 18515–18521

23 Randerson J T, Thompson M V, Malmstrom C M, et al. Substrate limitations for heterotrophs: Implications for models that estimate the seasonal cycle of atmospheric CO_2. Glob Biogeochem Cycle, 1996, 10: 585–602

24 Schimel D S, Braswell B H, Holland E A, et al. Climatic, edaphic, and biotic controls over storage and turnover of carbon in soils. Glob Biogeochem Cycle, 1994, 8: 279–293

25 Parton W J, Schimel D S, Cole C V, et al. Analysis of factors controlling soil organic matter levels in Great Plains grasslands. Soil Sci Soc Am J, 1987, 51: 1173–1179

26 Luo T X. Patterns of net primary productivity for Chinese major forest types and its mathematical models (in Chinese). Doctoral Dissertation. Beijing: Institute of Geographic Sciences and Natural Resources Research, Chines Academy of Sciences, 1996

27 Wang S, Zhou C, Li K, et al. Study on spatial distribution character analysis of the soil organic Carbon Reservoir in China. J Geogr Sci, 2001, 11: 3–13

28 Wang S, Tian H, Liu J, et al. Pattern and change of soil organic carbon storage in China: 1960s–1980s. Tellus Ser B-Chem Phys Meteorol, 2003, 55: 416–427

29 Yu G R, He H L, Liu X A, et al. Atlas for Spatialized Information of Terrestrial Ecosystem in China—Volume of Climatological Elements (in Chinese). Beijing: China Meteorological Press, 2004

30 Deng S Q. Map of Soil Texture of China. In: Institute of Soil Science, Chinese Academy of Sciences, ed. The Soil Atlas of China (in Chinese). Beijing: Cartographic Publishing House, 1986. 23–24

31 Haupt R L, Haupt S E. Practical Genetic Algorithms. 2nd ed. Hoboken: John Wiley & Sons Publication Inc, 2004

32 White L, Luo Y, Xu T. Carbon sequestration: inversion of FACE data and prediction. Appl Math Comput, 2005, 163: 783–800

33 Running S W, Thornton P E, Nemani R, et al. Global terrestrial gross and net primary productivity from the earth observing system. In: Sala O, Jackson R, Mooney H, eds. Methods in Ecosystem Science. New York: Springer-Verlag, 2000. 44–57

34 Zhu W Q, Pan Y Z, He H, et al. Simulation of maximum light use efficiency for some typical vegetation types in China. Chin Sci Bull, 2006, 51: 457–463

35 Peng S L, Guo Z H, Wang B S. Use of GIS and RS to estimate the light utilization efficiency of the vegetation in Guangdong, China (in Chinese). Acta Ecol Sin, 2000, 20: 903–909